

CoMFA-Based Prediction of Agonist Affinities at Recombinant D1 vs D2 Dopamine Receptors[†]

Richard E. Wilcox,^{*,‡,§} Tom Tseng,[‡] Mi-Youn Kim Brusniak,^{||} Brett Ginsburg,[‡] Robert S. Pearlman,^{||} Martha Teeter,[⊥] Curtiss DuRand,[∇] Stephanie Starr,[#] and Kim A. Neve[#]

Molecular Pharmacology Laboratory, College of Pharmacy, University of Texas at Austin, Austin, Texas 78712-1074, Institute for Neuroscience, University of Texas at Austin, Austin, Texas 78712, Laboratory for Molecular Graphics and Theoretical Modeling, College of Pharmacy, University of Texas at Austin, Austin, Texas 78712, Laboratory of Protein Modeling, Department of Chemistry, Boston College, Chestnut Hill, Massachusetts 02167, Psychiatry Service, VA Medical Center, Department of Veterans Affairs, Bedford, Massachusetts 01730, and Medical Research Service, Department of Veterans Affairs Medical Center, Portland, Oregon 97201

Received January 15, 1998

We have previously shown that using agonist affinity at recombinant receptors selectively expressed in clonal cells as the dependent variable in three-dimensional quantitative structure–activity relationship studies (3D-QSAR) presents a unique opportunity for accuracy and precision in measurement. Thus, a comparison of affinity's structural determinants for a set of compounds at two different recombinant dopamine receptors represents an attainable goal for 3D-QSAR. A molecular database of bound conformations of 16 structurally diverse agonists was established by alignment with a high-affinity template compound for the D1 receptor, 3-allyl-6-bromo-7,8-dihydroxy-1-phenyl-2,3,4,5-tetrahydro-1*H*-benzazepin. A second molecular database of the bound conformations of the same compounds was established against a second template for the D2 receptor, bromocriptine. These aligned structures suggested three-point pharmacophore maps (one cationic nitrogen and two electronegative centers) for the two dopamine receptors, which differed primarily in the height of the nitrogen above the plane of the catechol ring and in the nature of the hydrogen-bonding region. The $\ln(1/K_L)$ values for the low-affinity agonist binding conformation at recombinant D1 and D2 dopamine receptors stably expressed in C6 glioma cells were used as the target property for the CoMFA (comparative molecular field analysis) of the 16 aligned structures. The resulting CoMFA models yielded cross-validated R^2 (q^2) values (standard error of prediction) of 0.879 (1.471, with five principal components) and 0.834 (1.652, with five principal components) for D1 and D2 affinity, respectively. The simple R^2 values (standard error of the estimate) were 0.994 (0.323) and 0.999 (0.116), respectively, for D1 and D2 receptor. F values were 341 and 2465 for D1 and D2 models, respectively, with 5 and 10 df. The predictive utility of the CoMFA model was evaluated at both receptors using the dopamine agonists, apomorphine and 7-OH-DPAT. Predictions of K_L were accurate at both receptors. Flexible 3D searches of several chemical databases (NCI, MDDR, CMC, ACD, and Maybridge) were done using basic pharmacophore models at each receptor to determine the similarity of hit lists between the two models. The D1 and D2 models yielded different lists of lead compounds. Several of the lead compounds closely resembled high-affinity training set compounds. Finally, homology modeling of agonist binding to the D2 receptor revealed some consistencies and inconsistencies with the CoMFA-derived D2 model and provided a possible rationale for features of the D2 CoMFA contour map. Together these results suggest that CoMFA-homology based models may provide useful insights concerning differential agonist–receptor interactions at related receptors. The results also suggest that comparisons of CoMFA models for two structurally related receptors may be a fruitful approach for *differential QSAR*.

Introduction

Brain dopamine (DA) receptors regulate motor, endocrine, and emotional functions^{1–6} and are potentially

altered in neurological and psychiatric disorders and normal aging.^{7–9} Recently, several DA receptors, associated with D1 and D2 subfamilies, have been cloned.^{1,10–15} Determination of quantitative structure–activity relationship (QSAR) information on drug properties at D1 vs D2 DA receptors may lead to more selective ligands for each subfamily and to an improved understanding of the structural bases for agonist affinity. Those features of drug–receptor interactions which yield differences in affinity and efficacy at different DA

[†] Abbreviations: 7-OH-DPAT, (\pm)-2-dipropylamino-7-hydroxy-1,2,3,4-tetrahydronaphthalene; AAA, active analogue approach; ACD, Available Chemical Directory (114 471 compounds); ADTN, 2-amino-5,6-dihydroxy-1,2,3,4-tetrahydronaphthalene; APO, (*R*)-(-)-apomorphine; Br-APB, 3-allyl-6-bromo-7,8-dihydroxy-1-phenyl-2,3,4,5-tetrahydro-1*H*-3-benzazepin; Cl-APB, 3-allyl-6-chloro-7,8-dihydroxy-1-phenyl-2,3,4,5-tetrahydro-1*H*-3-benzazepin, SKF-82958; Cl-PB, 6-chloro-7,8-dihydroxy-1-phenyl-2,3,4,5-tetrahydro-1*H*-3-benzazepin; CMC, Comprehensive Medical Chemistry (5336 compounds); CoMFA, comparative molecular field analysis; DA, dopamine; D1 receptor, recombinant rhesus macaque D1 dopamine receptor; D2 receptor, recombinant rat D2_{short} dopamine receptor; DHX, dihydroxidine; EDTA, ethylenediaminetetraacetic acid; HEPES, *N*-[2-hydroxyethyl]piperazine-*N*-[2-ethanesulfonic acid]; K_L , low-affinity agonist dissociation constant, determined in C6 cells in the presence of GTP and sodium; MDDR, Modern Drug Data Report (51 119 compounds); Maybridge (49 811 compounds); NCI, National Cancer Institute (117 656 compounds); NPA, (*R*)-(-)-*N*-*n*-propylnorapomorphine; PPHT, 2-(*N*-phenylethyl-*N*-propyl)amino-5-hydroxytetralin; 3PPP, 3-(3-hydroxyphenyl)-*N*-propylpiperidine; QSAR, quantitative structure–activity relationship.

* To whom reprint requests may be directed. E-mail address for correspondence: wilcoxrich@mail.utexas.edu.

[‡] Molecular Pharmacology Laboratory, University of Texas at Austin.

[§] Institute for Neuroscience, University of Texas at Austin.

^{||} Laboratory for Molecular Graphics and Theoretical Modeling.

[⊥] Boston College.

[∇] Psychiatry Service, Department of Veterans Affairs.

[#] Medical Research Service, Department of Veterans Affairs Medical Center.

receptors may be extremely important in drug design.¹⁶ In turn, the development of subtype-selective drugs will improve the understanding of the role of DA receptor subtypes in brain physiology and disease.

A promising computational approach for direct study of drug features most closely associated with particular biological properties at a given receptor is comparative molecular field analysis (CoMFA),^{17–20} incorporating partial least squares (PLS) regression.²¹ Our previous work indicated that drug affinity data obtained at recombinant receptors may represent a significant improvement in deriving CoMFA models over more traditional target data obtained at native receptors in brain.²⁰ This suggests that CoMFA might reasonably be extended to a comparative evaluation of affinities for the same drug set at two closely related receptors (such as two DA receptor subtypes) to yield *differential* QSAR. Whereas in the brain the drugs of the training set may bind to confounding receptor sites, this is less likely for recombinant receptors appropriately expressed in a clonal cell line.^{5,22}

Initial conformations for training set compound alignment were established from CONCORD-derived structures²⁴ and minimized using the MAXIMIN2 procedure within SYBYL.²⁵ Typically, SYSTEMATIC or RANDOM search methods within SYBYL were employed to provide alternative starting conformations of reasonable energy. Subsequently, flexible field fit methods were used to determine the probable bound conformations of agonists at D1 and D2 receptors. Agonist binding affinities at recombinant D1 and D2 receptors stably expressed in C6 glioma or HEK293 cells were obtained for all training set compounds.²⁶ CoMFA was used to relate agonist affinities at the recombinant DA receptors to the steric and electrostatic fields of the aligned structures.^{19,20,27–28}

Methods

Measurement of Drug Affinity. A. Drug Affinity. C6 glioma or human embryonic kidney (HEK) 293 cells stably expressing either the rhesus macaque D1¹³ or rat D2-415 (D2 short)²⁹ receptor were grown and prepared for radioligand binding experiments as described previously.²⁶ Confluent cells were lysed by replacing the medium with ice-cold hypotonic buffer (1 mM Na⁺–HEPES, pH 7.0, 2 mM EDTA). After 10–20 min, the cells were scraped off the plate into centrifuge tubes and centrifuged at 17 000 rpm for 20 min. The crude membrane fraction was resuspended with a Brinkman polytron homogenizer (setting 6 for 10 s) in assay buffer (50 mM Tris-HCl, pH 7.4, 0.9% NaCl, 1 mM EDTA, 0.025% ascorbic acid, and 0.001% bovine serum albumin). Determination of agonist affinity was carried out in an assay volume of 250 μ L (D1) or 1 mL (D2), including cell membranes, radioligand (³H]-SCH23390, 2 nM for D1 assays or [³H]spiperone, 0.2 nM for D2 assays), GTP (100 μ M), and test drugs. GTP was added to shift the receptors to the low-affinity agonist binding conformation, which is the relevant conformation *in vivo*.³⁰ (+)-Butaclamol (2 μ M) was used to define nonspecific binding for both types of assay because of its high affinity for both receptors.³¹ Assay incubations were at 30 °C for 1 h and stopped by dilution with ice-cold wash buffer (10 mM Tris-HCl, pH 7.4, 0.9%

Table 1. Affinity and Energy of Compounds in the D1 and D2 Dopamine Receptor Training Sets

drug	K_L (μ M)		E_{conf} (kcal/mol)		E_{min} (kcal/mol)	
	D1	D2	D1	D2	D1	D2
ADTN	5.40	0.34	15.6	11.9	13.8	11.9
Br-APB	0.003	0.35	20.7	28.6	20.6	25.3
bromo	1.35	0.002	42.8	42.1	33.7	35.2
Cl-APB	0.02	0.51	29.0	26.8	30.0	26.8
Cl-PB	0.03	8.00	27.4	30.0	26.5	26.9
DA	18.20	7.94	19.1	18.0	15.9	14.6
DHX	1.20	1.70	27.2	25.0	20.5	19.8
fenoldopam	0.04	0.81	23.8	28.6	22.5	22.4
lisuride	0.077	0.0008	32.5	30.5	25.6	30.4
<i>m</i> -tyramine	48.00	20.00	15.9	11.6	10.8	11.6
NPA	1.51	0.05	31.4	36.1	25.7	26.7
<i>p</i> -tyramine	390.00	160.00	15.4	22.8	12.0	14.7
pergolide	2.02	0.05	51.5	39.3	39.9	38.9
PPHT	1.20	0.02	44.1	34.5	35.0	29.3
quinpirole	524.81	2.57	46.3	39.3	43.9	39.2
SKF38393	0.32	9.55	26.6	36.4	24.7	26.8

NaCl) and filtration with a Tomtec 96 well cell harvester. Samples were counted in a Wallac 1205 Beta-plate scintillation counter. Competition curves were analyzed by nonlinear regression using Prism (Graph-Pad Software, Inc.). Agonist affinities for D1 and D2 DA receptors are reported in Table 1.

B. Drugs and Reagents for the C6 Studies. DHX was a generous gift from Dr. Richard Mailman (University of North Carolina).³² 7-OH-DPAT, ADTN, bromocriptine, (+)-butaclamol, (*R*)-(-)-apomorphine, Cl-APB, Cl-PB, PPHT, 3PPP, quinpirole, SKF38393, lisuride, and pergolide were obtained from Research Biochemicals International (Natick, MA). [³H]SCH23390 was obtained from NEN and [³H]spiperone was from Amersham; other drugs and reagents were from Sigma Chemical Co.

C. Drug Affinities at Recombinant D1 and D2 Dopamine Receptors. The training set consisted of a structurally diverse set of 16 agonists for which stereochemical information is known and for which we had measured affinities.²⁶

Computational Chemistry. A. Pharmacophore Information. On the basis of site-directed mutagenesis studies^{22,26,35} and QSAR approaches^{16,33–34,36–38} the following pharmacophoric features were identified: (a) the distances of the catechol hydroxyl group oxygens or equivalent from the cationic nitrogen and (b) the height of the cationic nitrogen above the plane of the ring to which the hydroxyl oxygens or equivalent nitrogens are bonded. These general features do *not* assume a common pharmacophore map but merely recognize that certain portions of an agonist must be able to form electrostatic or hydrogen bonds to yield high affinity and efficacy. We obtained pharmacophore maps from the subset of aligned structures having K_L values less than 5 μ M at each receptor (see Table 1). For ergoline compounds in the training set, we aligned the cationic nitrogen, the nitrogen on the five-membered ring, and the aromatic six-membered ring. The affinity values given in micromolars were expressed as $\ln(1/K_L)$ because CoMFA fields represent the enthalpic aspect of the overall free energy of the drug–receptor interaction and the relationship between free energy and the equilibrium binding constant is logarithmic.

There are several caveats for building a receptor pharmacophore map from QSAR data. First, at best,

the map can only suggest possible receptor active-site conformations. Second, the model can reflect only those features which are identified as salient by the map. Thus, an incomplete pharmacophore map can cause the investigator to ignore crucial structural features. This is all the more likely when several structural classes of drugs are represented within the training set because the pharmacophore map may most heavily weight those drugs with structures most similar to that of the template compound. However, the advantages of a QSAR approach generally are that atomic positions of the presumed binding conformations are specified for each compound. Furthermore, for CoMFA-derived models key steric and/or electrostatic features of the aligned drugs which clearly reflect their *differences* in affinity are highlighted. Together, the apparent pharmacophoric features of the aligned "binding" conformations of the compounds provide a useful starting point for a CoMFA. Thus, the CoMFA begins with a pharmacophore map and extends the QSAR model beyond it.

B. Molecular Modeling: Initial Conformations and Template Selection. SYBYL 6.4²⁵ was used for the modeling in the present study. Initial structures were generated using either CONCORD (v3.0.1)^{24,36} or the cleanup procedure within SYBYL, geometrically optimized using the MNDO³⁸ procedure and minimized using MAXIMIN2. Ligands probably do not bind to the receptor in their global minimum energy conformations because some degree of torsional change or rotatable bond flexion is required to adapt the drug and receptor to electrostatic and hydrogen-bonding distances, yielding a drug-receptor complex of lower energy. Thus, the "minimum" energy conformation resulting from a MAXIMIN2 procedure is only a useful starting point for possible candidate conformations for the compound. However, it is important to restrict the possible conformations of the drugs to those which can reasonably be obtained upon binding. Typically, a 10 kcal/mol cutoff (difference between the local minimum and conformational energy) is considered reasonable.^{42,47}

Identification of possible candidate conformations for the majority of training set compounds had been previously accomplished using the MULTISEARCH procedure within the SYBYL DISCO module or the RANDOM and SYSTEMATIC search features of SYBYL.³⁸⁻⁴¹ As necessary, these latter procedures were repeated to assist in optimizing the alignment with the template to identify a reasonable set of candidate conformations of each molecule that are within the region of conformation space (i.e., distance space) accessible to all of the compounds. Such conformations are a useful starting point for flexible field fit procedures that optimize the alignment and conformations of the compounds of the training set.

Compound alignment is, of course, required both for pharmacophore map determination and as a necessary prelude to CoMFA. Two requirements need to be met: (a) determination of a specific "bound" conformation and (b) alignment of all chosen conformations in a common orientation relative to a template compound. We selected Br-APB as the template for determining the bound conformation of the flexible ligands at the D1 receptor because it is a reasonably constrained drug with high D1 receptor affinity⁵⁴ (Table 1).⁶⁰ Similarly,

we selected bromocriptine as the template for drug alignment at the D2 receptor (Figure 1).

In the present study we used the same set of 16 agonists for two parallel CoMFAs to predict affinity at D1 and D2 receptors. This was crucial to achieve the goals of the present work since a major objective was to compare D1 and D2 CoMFA models directly. In the first analysis, drug alignment was with Br-APB and the CoMFA model was optimized for prediction of drug affinity at the D1 receptor. In the second analysis, alignment of the same 16 compounds used bromocriptine as the template and the drug alignment and CoMFA model were optimized for predicting drug affinity at the D2 receptor.

C. Alignment. Alignment of the presumed bound conformations of the training set compounds is the other essential prelude to CoMFA (in addition to selection of an appropriate template compound/conformation). There are several field fit procedures available for conformer selection and/or modification and alignment.^{17-20,27,28,41} A flexible field fit method was used in the present study. Following the flexible field fit, MOPAC charges were recalculated and the conformational energy of the compound was obtained. For some compounds for each CoMFA, the flexible field fit procedure was not found to improve the alignment of the compounds relative to a simple fitting of atoms. In those instances, the initial alignment was retained. For the initial flexible field fit at each receptor, the electrostatic and steric fields used for the template compound were based on the initial and default CoMFA run and the CoMFA region used for these field fits was that associated with the same CoMFA run. Following CoMFA model optimization at each receptor, the flexible field fit procedures were repeated using the CoMFA region from the optimum run and the electrostatic and steric fields for the template associated with that model to further verify it.

D. CoMFA. Partial least squares regresses a target property (e.g., $\ln(1/K_L)$) against predictors calculated as steric and electrostatic components of the intermolecular interaction field. These are evaluated at the grid points of a three-dimensional lattice containing each member of a training set of aligned ligand structures. In the present study "grid boxes" were generated for alignments based on the Br-APB or bromocriptine templates. As discussed,^{17,18,20} we have systematically investigated the effects of changing several CoMFA parameters, including grid step size (1.5–2.5 Å), probe atom type (H^+ , O^- , $C_{sp^3}^+$), and the column filtering values (≈ 1.0 –4.0 kcal/mol). We used the "leave one out" method for cross-validation.²⁵

3D-Search of Chemical Databases. One useful way to compare potentially different CoMFA models is to perform flexible 3D searches of large chemical databases for potential "lead" compounds which possess the desired features.⁴⁴ Here, we used the UNITY software accessible through SYBYL (version 2.6) to perform searches of the following databases: NCI, MDDR, ACD, CMC, and Maybridge. The first D1 query used in each instance was a simple pharmacophore representing distances between the cationic nitrogen and the meta and para hydroxyls plus the separation between hydroxyls. Distance constraints were based on

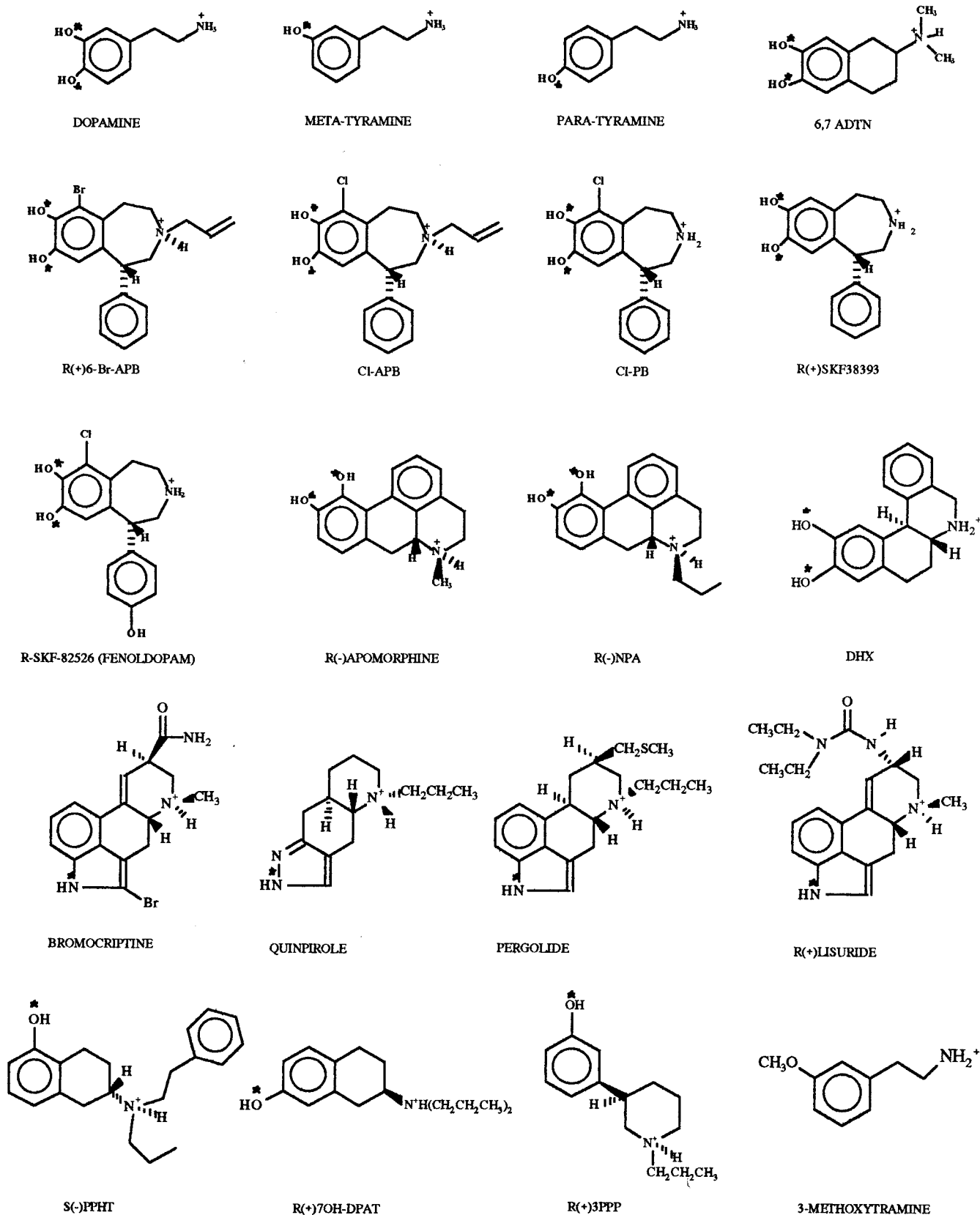


Figure 1. Structures of drugs in the training and test sets. * Refers to groups used in establishing the pharmacophore map.

the highest D1 affinity compounds in the set (Br-APB, Cl-APB, Cl-PB, and fenoldopam).²⁶ Similarly, the initial D2 query was based on the distances between the cationic nitrogen and the nitrogen of the five-membered ring (in a position analogous to that of the meta hydroxyl of catechols) and between the cationic nitrogen

and the carbon adjacent to the bromine of that ring. The three highest D2 affinity ergoline compounds (bromocriptine, lisuride, and pergolide) were used to set the constraints for this set of searches.²⁶ A second stage of 3D searching was then carried out on the five hit lists for the D2 query. In this instance, the simple pharma-

cophoric queries were modified to include features from the actual CoMFA model (exclusion volume), and only the initial hit lists were searched to find potential best hits.

Docking of Agonists into D2 Receptor Model.

The protein homology model used here for docking was essentially that developed for the D2 receptor by two of the coauthors.³⁷ In brief, it was based on the experimentally obtained three-dimensional bacteriorhodopsin structure and D2 receptor ligand binding mutagenesis data. These data were used to align rhodopsin with bacteriorhodopsin. Alignment of low-homology sequences was aided by establishing polar and nonpolar faces via helical wheels. From the alignment, D2 residues were substituted into the Protein Data Bank coordinates of bacteriorhodopsin to (entry lbrd) build an initial databased D2 model. Local geometry optimization, Pro replacements, and side chain rotation consistent with protein structure knowledge refined this model. Global energy minimization was not used for the final model for the reasons discussed.³⁷ A more detailed discussion of this methodology is contained in the Methods section of ref 37.

Four D2 agonists (bromocriptine, lisuride, pergolide, and dopamine) in the CoMFA alignment derived here were docked into the dopamine D2 receptor homology-based model as we have previously published.³⁷ As a first approximation, the model was not changed from the model described in the paper. Target points for the docking were the Asp in helix 3 and the Ser residues on helix 5, as previously described.^{37,39} Since bromocriptine had only one of the hydrophilic groups (the nitrogen in the five-membered ring) which corresponded to the meta hydroxyl of dopamine, optimal docking to only one Ser hydroxyl of the receptor was possible, but the second Ser could form a longer hydrogen bond with the nitrogen.

Results

Drug Affinity. Membrane D1 and D2 agonist affinity was determined in C6 glioma or HEK293 cells expressing the recombinant receptor (Table 1). Assays were conducted in the presence of saturating GTP and physiological NaCl and without Mg²⁺ to prevent coupling of the receptors to G proteins. Hill coefficients for competition binding curves did not differ significantly from unity (data not shown). Of the 16 initial training set compounds, 5 had more than 10-fold selectivity for D1 receptors, 7 were selective for D2 receptors, and 4 were relatively nonselective. Affinity values (K_L) ranged from 2–3 nM for Br-APB and bromocriptine at D1 and D2 receptors, respectively, to 200–400 μ M for *p*-tyramine at both receptor subtypes. Lisuride and pergolide had subnanomolar K_L at D2 receptors (Table 1).

Computational Chemistry. A. Two-Dimensional Structures and Alignment of the Training Set Compounds. The D1 and D2 training set (Figure 1)^{26,48,49} compounds had final conformational energy (E_{conf}) within 10 kcal/mol of the local minimum (E_{min} , Table 1). Pharmacophore maps were obtained from the subset of aligned structures having K_L values less than 5 μ M at each receptor (Figure 2). Flexible field fit procedures were used to determine the final alignments

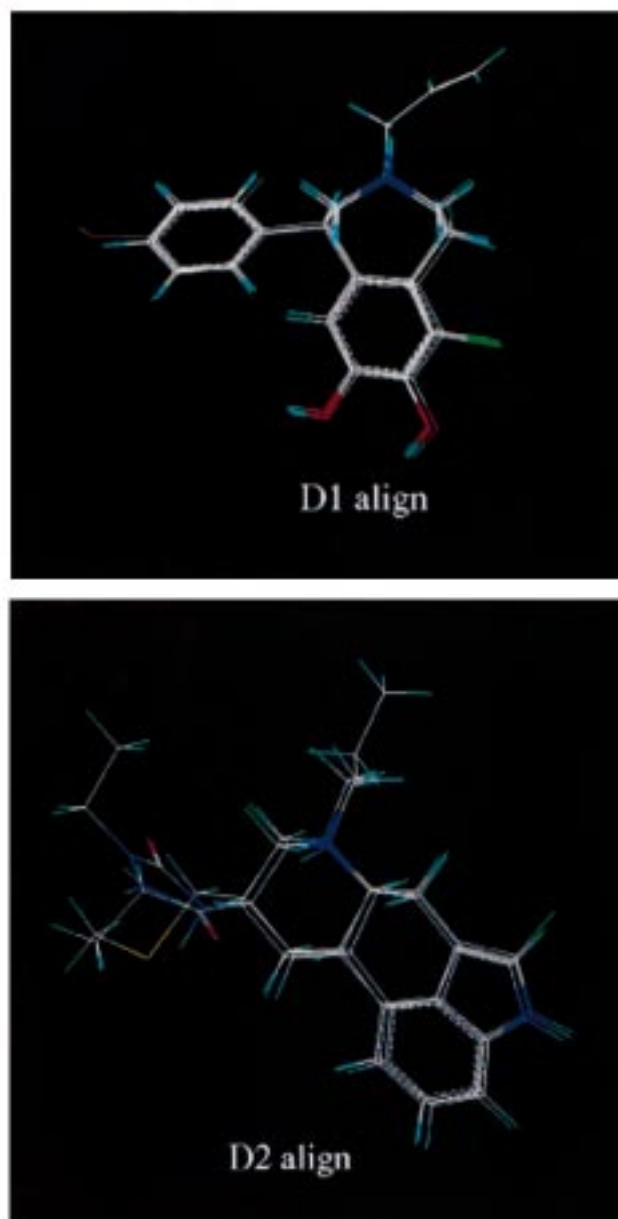


Figure 2. Structures of the aligned drugs of the training set. Top panel: alignment with DHX for D1 receptor affinity. Bottom panel: alignment with bromocriptine for D2 affinity.

of and conformations of compounds in the training sets. The final alignments for the D1 and D2 training sets are highlighted in Figure 2, using Br-APB (top panel) and bromocriptine (bottom panel) as the templates for the D1 and D2 receptors, respectively. Although all compounds were aligned in each instance, for clarity only the compounds possessing the highest affinity for each receptor are shown in the respective panels of the figure.⁶¹ While the alignments are different for the D1 and D2 models, in both the importance of the cationic nitrogen and hydrogen bonding regions is apparent.

B. Pharmacophore Maps for Affinity at Dopamine Receptors. Pharmacophore maps based on the highest affinity compounds in the training set are shown in Figure 3 (panels A and B) and Tables 2 and 3, respectively, for D1 and D2 models. At the D1 receptor and for the compounds with highest affinity and greatest D1 selectivity (Br-APB, Cl-APB, Cl-PB, and fenoldopam), the distance between the cationic nitrogen

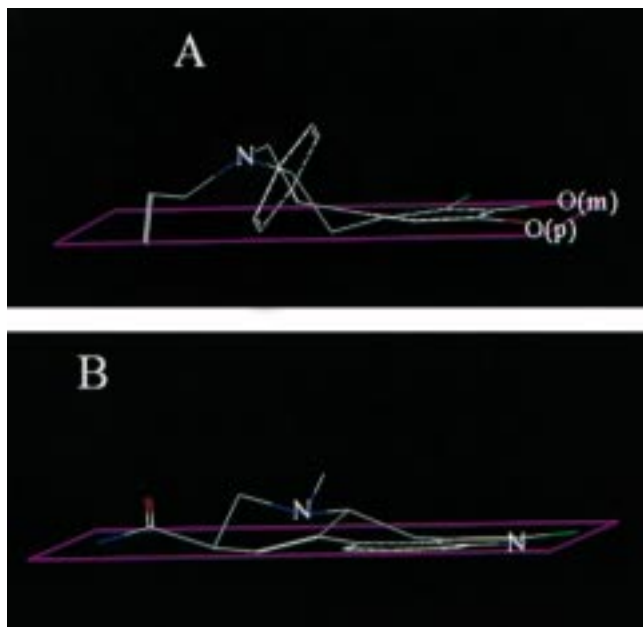


Figure 3. Pharmacophore map for high-affinity drugs of the training set.

Table 2. Pharmacophore Map for Agonists at the D1 Dopamine Receptor^a

compd	N- <i>m</i> -OH (Å)	N- <i>p</i> -OH (Å)	N-plane height (Å)
ADTN	7.7	7.3	1.51
Br-APB	6.97	6.7	1.28
bromo	5.1	5.9	0.51
Cl-APB	6.9	6.7	1.32
Cl-PB	7.0	6.8	1.24
DA	7.8	7.5	1.46
DHX	7.5	7.1	2.07
fenoldopam	7.0	6.8	1.25
lisuride	5.9	5.1	0.63
<i>m</i> -tyramine	7.5		1.06
NPA	7.8	6.5	1.44
<i>p</i> -tyramine		7.9	1.11
pergolide	5.9	5.1	0.63
PPHT	6.6		1.01
quinpirole	5.9	5.6	0.54
SKF38393	7.0	6.8	1.35

^a Bold indicates the compounds with the highest affinity and greatest D1 selectivity.

and the meta hydroxyl oxygen ranged from 6.9 to 7.0 Å (panel A, distance A). At the D2 receptor the distance between the carbon of the five-membered ring meta to the cationic nitrogen and the cationic nitrogen was 5.1 Å for the highest affinity and D2-selective ergoline compounds (bromocriptine, lisuride, pergolide; panel B, distance A) and from 6.6 to 7.6 Å for NPA and PPHT. Thus, distances between these two pharmacophoric elements were generally similar for the two receptors. At the D1 receptor, the distance between the cationic nitrogen and the para hydroxyl oxygen ranged from 6.7 to 6.8 Å (panel A, distance B) for the high-affinity and D1-selective compounds. At the D2 receptor the distance between the para hydroxyl (or nitrogen of the five-membered ring para to the cationic nitrogen) and the cationic nitrogen was 6.0 Å for the three high-affinity, D2-selective ergoline compounds (panel B, distance B) and 6.4 Å for NPA. Thus, although there is overlap for the distance between the cationic nitrogen and hydrogen-bonding group in the para position for D1 and D2

Table 3. Pharmacophore Map for Agonists at the D2 Dopamine Receptor^a

compd	N- <i>m</i> -OH (Å)	N- <i>p</i> -OH (Å)	N-plane height (Å)
ADTN	7.8	7.4	0.50
Br-APB	7.0	6.8	1.17
bromo	5.1	6.0	0.44
Cl-APB	7.0	6.7	1.22
Cl-PB	7.0	6.9	1.04
DA	8.0	6.9	0.73
DHX	7.8	7.3	0.34
fenoldopam	7.0	6.8	1.10
lisuride	5.1	6.0	0.39
<i>m</i> -tyramine	7.6		1.48
NPA	7.6	6.4	1.83
<i>p</i> -tyramine		7.8	1.40
pergolide	5.1	6.0	0.61
PPHT	6.6		0.16
quinpirole	6.0	5.6	0.44
SKF38393	6.6	6.6	1.19

^a Bold indicates the highest affinity and D2-selective ergoline compounds.

agonists, the distance appears slightly greater for optimal D1 affinity.

A pharmacophore map feature which had been hypothesized to differentiate between the D1 and D2 receptors²⁰ was the cationic nitrogen height above the plane of the catechol (or heteroatom-containing 5C) ring. For the high-affinity compounds in the Br-APB-D1 alignment (Table 2), this height was 1.24–1.32 Å (Figure 3, panel A, distance C). The plane heights for the three D2 high-affinity ergoline compounds in the bromocriptine-D2 alignment ranged from 0.39 to 0.61 Å (Figure 3, panel B, distance C). For NPA and PPHT, the plane heights were 1.83 and 0.16 Å, respectively, for the D2 receptor pharmacophore map (Table 3). For DA itself, the plane heights were found to be 1.46 Å for the D1 conformer and 0.73 Å for the D2 conformer. Interestingly, every training set compound except NPA, SKF38393, and the two tyramine isomers had a higher plane height in the D1 map than in the D2 map. Some of these, in addition to DA, are quite dramatically different—ADTN, DHX, PPHT, lisuride. Thus, with few exceptions, the present results support the relevance of the distinction for this pharmacophoric feature. It is emphasized that pharmacophore maps based on flexible field fit procedures are most useful as starting points for CoMFA rather than as describing by themselves all essential features of a drug–receptor interaction model.

C. Comparative Molecular Field Analysis. C.1. CoMFA for Agonist Affinity at the D1 DA Receptor. The cross-validated R^2 (q^2) values which resulted from the various CoMFA options for K_L at recombinant D1 and D2 receptors as the target property are shown in Tables 4 and 5, respectively. Using the default CoMFA settings, which included both steric and electrostatic fields, we observed a standard error of prediction (SEP) of 2.430 with five principal components and a q^2 of 0.670 for agonist affinity at the D1 DA receptor (Table 4).⁶² The choice of CoMFA options described below was based both on maximizing the q^2 value and minimizing SEP.^{18,20} The final model, without cross-validation and with five principal components, was obtained using the following options: steric and electrostatic fields with 7.5 kcal/mol cutoffs, $1/r$ for the dielectric function, a 2.0 Å step size, 2.0 kcal/mol column filtering, a C_{sp3+} probe atom, and a grid box set at

Table 4. CoMFA Results for D1 Dopamine Receptor Using Br-APB as Template ($N = 16$)

field type	cutoff energy (kcal/mol)	dielec function	CoMFA region	min σ	grid step size (Å)	probe atom type	q^2 (no. comp)
both ^a	30	1/ <i>r</i>	default	2.0	2.0	C _{sp3} ⁺	0.670 (5)
both	30	1.0	default	2.0	2.0	C _{sp3} ⁺	0.543 (4)
steric	30	1/ <i>r</i>	default	2.0	2.0	C _{sp3} ⁺	0.716 (5)
electro ^b	30	1/ <i>r</i>	default	2.0	2.0	C _{sp3} ⁺	0.768 (5)
both	10	1/ <i>r</i>	default	2.0	2.0	C _{sp3} ⁺	0.803 (5)
both	50	1/ <i>r</i>	default	2.0	2.0	C _{sp3} ⁺	0.608 (5)
steric	10	1/ <i>r</i>	default	2.0	2.0	C _{sp3} ⁺	0.749 (5)
steric	50	1/ <i>r</i>	default	2.0	2.0	C _{sp3} ⁺	0.699 (5)
electro	10	1/ <i>r</i>	default	2.0	2.0	C _{sp3} ⁺	0.742 (5)
electro	50	1/ <i>r</i>	default	2.0	2.0	C _{sp3} ⁺	0.715 (5)
both	20	1/ <i>r</i>	default	2.0	2.0	C _{sp3} ⁺	0.608 (1)
both	5	1/ <i>r</i>	default	2.0	2.0	C _{sp3} ⁺	0.674 (3)
both	15	1/ <i>r</i>	default	2.0	2.0	C _{sp3} ⁺	0.613 (1)
both	7.5	1/ <i>r</i>	default	2.0	2.0	C _{sp3} ⁺	0.879 (5)
both	S10/E7.5 ^c	1/ <i>r</i>	default	2.0	2.0	C _{sp3} ⁺	0.847 (5)
both	S7.5/E10	1/ <i>r</i>	default	2.0	2.0	C _{sp3} ⁺	0.795 (5)
both	7.5	1/ <i>r</i>	default	2.0	1.5	C _{sp3} ⁺	0.729 (3)
both	7.5	1/ <i>r</i>	default	2.0	2.0	H ⁺	0.744 (3)
both	7.5	1/ <i>r</i>	default	2.0	2.0	O ₃ ⁻	0.759 (2)
both	7.5	1/ <i>r</i>	default	2.5	2.0	C _{sp3} ⁺	0.729 (4)
both	7.5	1/ <i>r</i>	default	1.5	2.0	C _{sp3} ⁺	0.783 (5)
both	7.5	1/ <i>r</i>	default	1.9	2.0	C _{sp3} ⁺	0.874 (4)
both	7.5	1/ <i>r</i>	default	1.85	2.0	C _{sp3} ⁺	0.879 (4)
both^d	7.5	1/<i>r</i>	default	2.0	2.0	C_{sp3}⁺	0.879 (5)

^a Steric and electrostatic. ^b Electrostatic. ^c Steric/electrostatic. ^d Bold indicates the options used for the final model.

Table 5. CoMFA Results for D2 Dopamine Receptor Using Bromocriptine as Template ($N = 16$)

field type	cutoff energy (kcal/mol)	dielec function	CoMFA region	min σ	grid step size (Å)	probe atom type	q^2 (no. comp)
both ^a	30	1/ <i>r</i>	default	2.0	2.0	C _{sp3} ⁺	0.792 (5)
both	30	1.0	default	2.0	2.0	C _{sp3} ⁺	0.756 (5)
steric	30	1/ <i>r</i>	default	2.0	2.0	C _{sp3} ⁺	0.706 (5)
steric	10	1/ <i>r</i>	default	2.0	2.0	C _{sp3} ⁺	0.619 (5)
steric	50	1/ <i>r</i>	default	2.0	2.0	C _{sp3} ⁺	0.700 (5)
electro ^b	30	1/ <i>r</i>	default	2.0	2.0	C _{sp3} ⁺	0.609 (5)
electro	50	1/ <i>r</i>	default	2.0	2.0	C _{sp3} ⁺	0.641 (5)
both	50	1/ <i>r</i>	default	2.0	2.0	C _{sp3} ⁺	0.783 (5)
both	10	1/ <i>r</i>	default	2.0	2.0	C _{sp3} ⁺	0.800 (5)
both	20	1/ <i>r</i>	default	2.0	2.0	C _{sp3} ⁺	0.807 (5)
both	25	1/ <i>r</i>	default	2.0	2.0	C _{sp3} ⁺	0.806 (5)
both	15	1/ <i>r</i>	default	2.0	2.0	C _{sp3} ⁺	0.820 (5)
both	17.5	1/ <i>r</i>	default	2.0	2.0	C _{sp3} ⁺	0.814 (5)
both	S15/E10 ^c	1/ <i>r</i>	default	2.0	2.0	C _{sp3} ⁺	0.814 (5)
both	S15/E20	1/ <i>r</i>	default	2.0	2.0	C _{sp3} ⁺	0.802 (5)
both	S15/E12.5	1/ <i>r</i>	default	2.0	2.0	C _{sp3} ⁺	0.833 (5)
both	S15/E12.5	1/ <i>r</i>	default	2.5	2.0	C _{sp3} ⁺	0.834 (5)
both	S15/E12.5	1/ <i>r</i>	default	1.5	2.0	C _{sp3} ⁺	0.815 (5)
both	S15/E12.5	1/ <i>r</i>	default	2.1	2.0	C _{sp3} ⁺	0.834 (5)
both	S15/E12.5	1/ <i>r</i>	default	2.1	2.5	C _{sp3} ⁺	0.753 (5)
both	S15/E12.5	1/ <i>r</i>	default	2.1	1.5	C _{sp3} ⁺	0.829 (5)
both	S15/E12.5	1/ <i>r</i>	default	2.1	2.0	H ⁺	0.792 (5)
both	S15/E12.5	1/ <i>r</i>	default	2.1	2.0	O ₃ ⁻	0.816 (5)
both	S15/E12.5	1/<i>r</i>	default	2.1	2.0	C_{sp3}⁺	0.834 (5)

^a Steric and electrostatic. ^b Electrostatic. ^c Steric/electrostatic. ^d Bold indicates the options used for the final model.

SYBYL's default position. This model had a q^2 value of 0.879 with five principal components, a SEP of 1.471, an R^2 value of 0.994, and a standard error of estimate (SEE) of 0.323. This yielded an $F(5, 10)$ of 341. The final cross-validated model utilized 83 of 1980 columns in the analysis. Figure 4, panel A, shows the relationship between calculated and measured K_L values for the non-cross-validated D1 analysis. For the D1 CoMFA, the residual values for the non-cross-validated analysis ranged from -0.480 for Cl-APB to 0.531 for ADTN (not shown).

C.2. CoMFA for Agonist Affinity at the D2 DA Receptor. Using the default CoMFA settings, we observed a SEP of 1.852 with five principal components and a q^2 of 0.792 for D2 agonist affinity (Table 5). The

final non-cross-validated model had a q^2 value of 0.834 with five principal components, a SEP of 1.652, and utilized 286 of 2178 columns in the analysis. This model was obtained using the following options: both steric and electrostatic fields (with 15 and 12.5 kcal/mol cutoff values respectively), 1/*r* for the dielectric function, a 2.0 Å step size, a 2.1 kcal/mol column filtering, a C_{sp3}⁺ probe atom, and a grid box set at SYBYL's default position. The non-cross-validated final model had an R^2 value of 0.999 with a SEE of 0.116 using five principal components. This analysis yielded an $F(5, 10)$ of 2465. Figure 4, panel B, shows the relationship between actual $\ln(1/K_L)$ values in micromolars for the training set compounds and the values predicted by the CoMFA model for the non-cross-validated (R^2) D2 analysis. For the

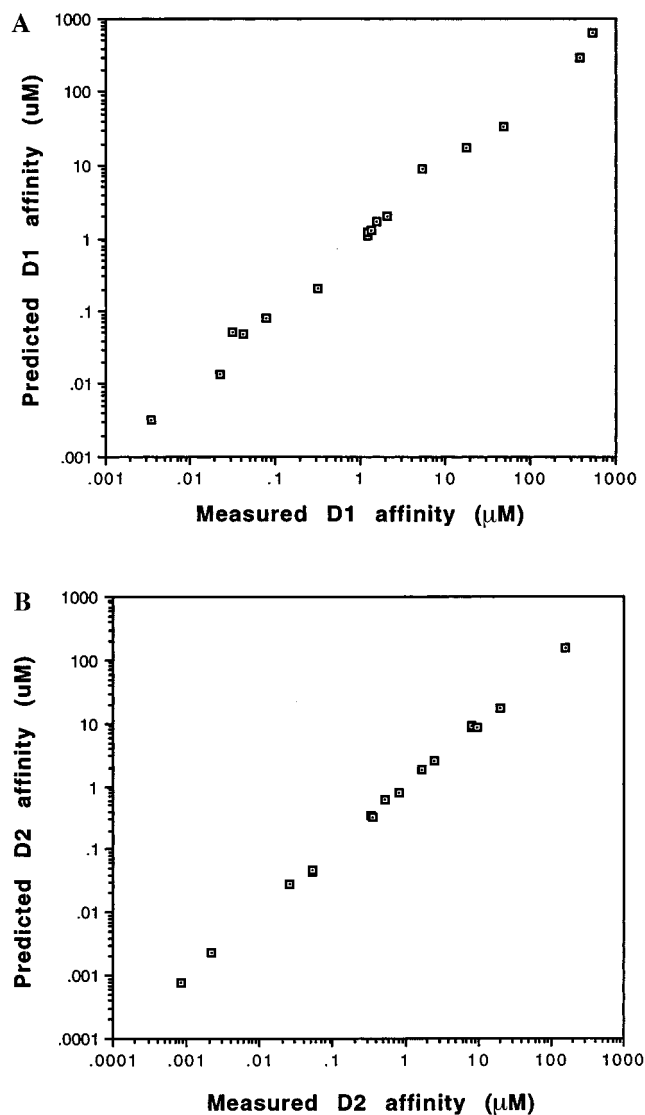


Figure 4. Relationship between measured and predicted affinity values at recombinant DA receptors for the compounds of the training set. Panel A: relationship at recombinant D1 DA receptors. Panel B: relationship at recombinant D2 DA receptors.

D2 CoMFAs, the residual values for the non-cross-validated analysis ranged from -0.154 for NPA to 0.170 for Cl-APB (not shown). Thus, for neither D1 nor D2 CoMFA models was there an obvious association between drug affinity or structural class and the residual value.

D. Contour Map. Figure 5 shows the contour map of the final D1 CoMFA model. Both steric and electrostatic fields were utilized, since this improved the SEP and the q^2 value over alternative models. Figure 6 shows the contour map of the final D2 CoMFA model. As with the D1 model, for the final D2 CoMFA model both electrostatic and steric fields were utilized. Furthermore, incorporation of similar features in both models facilitated a direct comparison between their features. The two contour maps show several potentially important differences. First, the D1 map does not exhibit any striking electrostatic features in the vicinity of the cationic nitrogen, suggesting that differences among the training set compounds in this region of the molecule are not of major importance (Figure 5). In

contrast, the D2 map does show a region somewhat near the cationic nitrogen in which positive charge favors high affinity at the D2 receptor. This suggests that the side groups, especially of the ergoline compounds, may play an important role in binding affinity relative to the catecholamine type compounds of the training set (Figure 6). A second difference is that steric bulk favors high affinity for the D2 receptor in a region near the cationic nitrogen (Figure 6) but not for a similar position in relation to the cationic nitrogen at the D1 receptor (Figure 5). A third difference is that only in the D2 map is there a region in which positive electrostatic charge is unfavorable for high affinity (near the center of the molecule in Figure 6). Perhaps the most striking similarity between the two contour maps lies in the hydrogen-bonding regions. Both D1 and D2 maps show regions in which positive electrostatic charge favors high affinity. In the D1 map (Figure 5), this is near the meta hydroxyl whereas in the D2 map it is near the hydrogen-bonding nitrogen of the five-membered ring (Figure 6). Finally, one of the more generally interesting features of any CoMFA-derived contour map is the region in which steric bulk is unfavorable for high affinity. Each of the two contour maps shown in Figures 5 and 6 defines a region of space in which significant steric hindrance would occur (exclusion volume).

E. Predictive Abilities of the CoMFA Models.

Using the procedures described in the Methods section, the affinities of two test compounds, *not* in the training set, at recombinant D1 and D2 receptors stably expressed in C6 glioma cells were obtained in the presence of sodium and GTP (Table 1).²⁶ Conformers for APO and 7-OH-DPAT were generated using RANDOM or SYSTEMATIC search procedures within SYBYL. From the sets of conformers, representative ones were selected which varied in their energy and with pharmacophoric features similar to those of the respective templates. Each was fit to the template using the FIT ATOMS routine within SYBYL. The measured D1 K_L value for APO was $0.22 \mu\text{M}$ whereas the predicted value was $0.24 \mu\text{M}$; for 7-OH-DPAT the measured value was $13.0 \mu\text{M}$, while the predicted value was $17.9 \mu\text{M}$. For D2 affinities the measured value for APO was $1.19 \mu\text{M}$ while the predicted value was $1.07 \mu\text{M}$; for 7-OH-DPAT the measured value was $0.94 \mu\text{M}$ while the predicted value was $0.85 \mu\text{M}$.⁶³

Predictive Abilities of the Pharmacophore Maps and CoMFA Models via 3D Database Searching.

The UNITY program (version 2.6) which can be used either independently, or within SYBYL,²⁵ was utilized to perform flexible 3D searches of several chemical databases in two stages for each database. First, simple 3D search queries were formulated using distances based on the highest affinity compounds in the training set for each receptor, and flexible 3D searches were conducted. Initially, the queries were validated against the training set compounds. As shown in Table 6A, the D1 query yielded Br-APB, Cl-APB, Cl-PB, fenoldopam, and DA from the training set. The D2 query yielded bromocriptine, lisuride, and pergolide from the training set. Thus, each query yielded the compounds used to generate it. Each search generated more than 100 hits of potential lead compounds (Table 6B). Importantly, the intersection of the hit lists for each database derived



Figure 5. Contour map of electrostatic field (standard deviation times coefficient) from D1 CoMFA model with the template compound Br-APB. Positive electrostatic charge is favored (blue) or unfavored (red) for high affinity. Steric bulk is favored (green) or unfavored (yellow) for high affinity.

from D1- and D2-based queries was obtained and yielded from 0 to 5 common hits (Table 6B, third column), which is <5% of the corresponding hit lists.⁶⁴

Second, the D2 search query was refined to include exclusion volumes using information based on the steric features of the D2 CoMFA model, and the search-generated databases were reexamined (Figure 8 vs Figure 7; Table 6B, second column, bracketed values). In each instance, use of the exclusion volume as a part of the query greatly reduced the number of potential hits. Finally, similarity searches of each hit list were performed to the highest affinity compounds of the training set (similarity to Br-APB for D1 hit lists and lisuride for D2 hit lists). Table 7 provides compound descriptors and similarity indices. Note especially that the similarity comparison of the D1-CMC hit list yielded fenoldopam and the D2-MDDR comparison with lisuride yielded two compounds (Figure 9) which are lisuride enantiomers.⁶⁵

Protein Homology Modeling of Agonist Binding to D2 Receptors. Protein homology modeling provides an independent approach for determining the basis of binding and stabilization of ligands and identifies residues of the receptor as candidates for interaction with specific atoms of ligands. This second feature suggests experiments to test interacting residues and to alter affinity by making specific structural changes in ligands. The protein homology model of the D2 DA receptor used here was that previously developed by us.³⁷ For the docked D2 agonists (dopamine, lisuride, pergolide, and bromocriptine; see Methods section), we examined both the *common* D2 pharmacophore in relation to the receptor model and the differences in the

ligands which might account for the different binding affinities. The pharmacophore was examined first and is in reasonable agreement with our previously published agonist dockings.^{37–39} In particular, the distance between the cationic nitrogen of the agonists to helix 3 Asp 114 was 3–3.2 Å. (Figure 10; numbers used here are for D2 short). The distance of the bromocriptine nitrogen in the five-membered ring to Ser 194 was 3.19 Å. The distance of the meta hydroxyl of dopamine to Ser 194 was 2.55 Å, while the distance of the para hydroxyl to Ser 194 was 3.32 Å. Dopamine is docked in an orientation rotated 180° from that previously published (Figure 11A).³⁷ Comparing the two dopamine dockings indicates that the current dopamine docking places the meta hydroxyl of dopamine in the same space as that of meta hydroxyl from the 1994 publication. However, although the para hydroxyl groups in the two dockings are far apart, the cationic nitrogen atoms are superimposed. In the docking presented here, *both* dopamine hydroxyls are within hydrogen-bonding distance of Ser194. Dopamine's long distance of 8.52 Å to Trp 116, which lines the receptor pocket, shows that dopamine does *not* fit tightly in the binding site. This might explain its binding affinity, which is lower than that of most of the other agonists in the training set.

Lisuride (Figure 11B) contains a diethyl urea group (see also Figure 1). The tertiary nitrogen has potential contacts with Tyr 379, Thr 383, and Tyr 387 of helix 7 with distances of 3–3.8 Å (Figure 11B).⁶⁶ Tyr 387 is an important residue in helix 7, which corresponds to the site of retinal attachment in the homologous G protein coupled receptor rhodopsin and the distantly related protein bacteriorhodopsin. This potentially

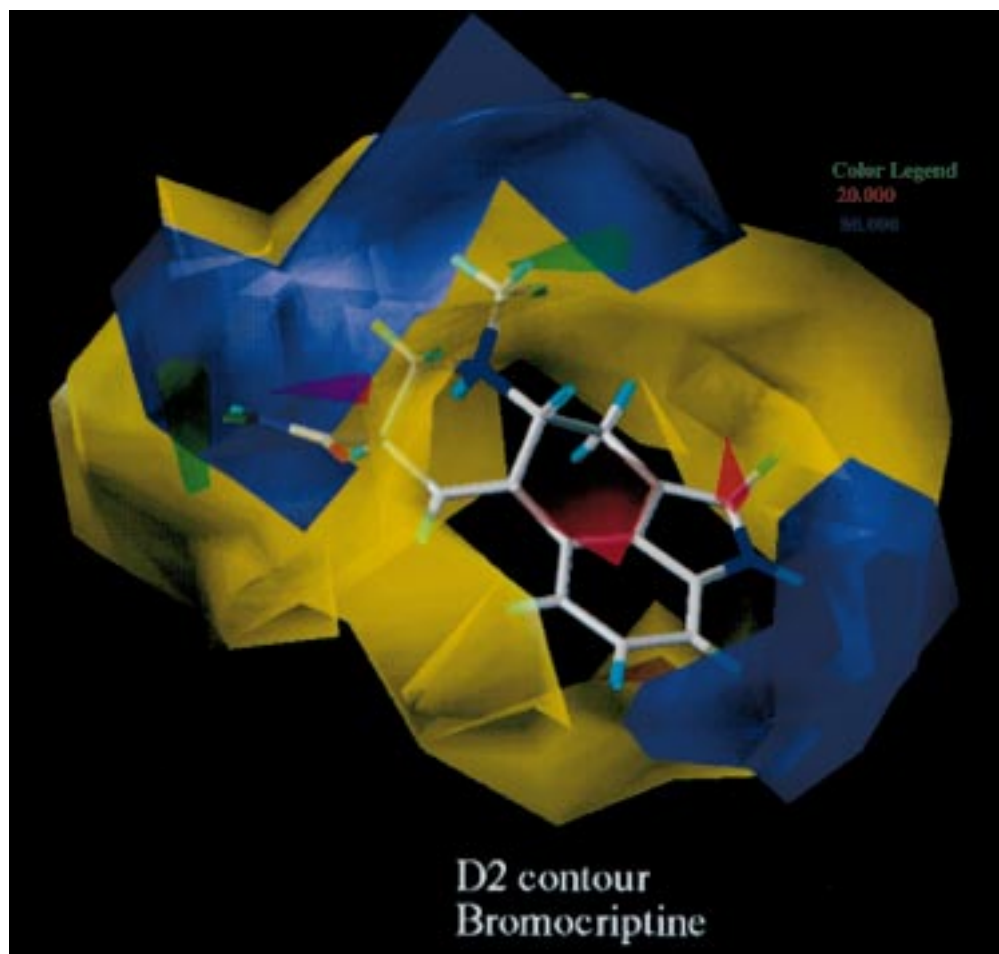


Figure 6. Contour map of electrostatic field (standard deviation times coefficient) from D2 CoMFA model with the template compound bromocriptine. Positive electrostatic charge is favored (blue) or disfavored (red) for high affinity. Steric bulk is favored (green) or disfavored (yellow) for high affinity.

Table 6. 3D Search Results

A. Results for Training Set		
check D1 query via flex. 3D search (hits given below) ^a	check D2 query via flex. 3D search (hits given below)	
Br-APB	bromo	
Cl-APB	lisuride	
Cl-PB	pergolide	
fenoldopam		
dopamine		
B. Results for 3D Databases		
query/database (hits) D1 query	query/database (hits) D2 query [exclusion volume hits]	intersection of D1 & D2 queries, common hits
NCI (383) ^b	NCI (311) [38]	4
MDDR 1004)	MDDR (373) [45]	3
ACD (379)	ACD (1099) [30]	0
CMC (112)	CMC (135) [6]	5
Maybridge (170)	Maybridge (437) [11]	4

^a Hits in columns 1 and 2 of Table 6A are from the training sets. ^b ACD, Available Chemical Directory (114 471 compounds); CMC, Comprehensive Medical Chemistry (5336 compounds); MDDR, Modern Drug Data Report (51 119 compounds); Maybridge (49 811 compounds); NCI, National Cancer Institute (117 656 compounds).

favorable contact, along with those for the other helix 7 residues, could explain the increased affinity of lisuride vs the other three agonists tested in this portion of the study. Further, this could represent an unusual stabilization feature that is not hypothesized for analy-

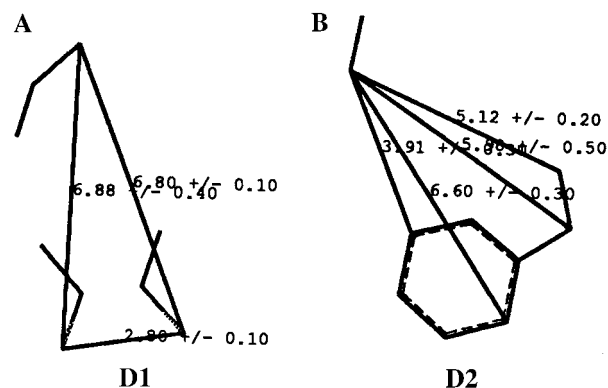


Figure 7. 3D search queries for six 3D chemical databases. Panel A: D1 search query. Panel B: D2 search query.

sis by CoMFA (i.e., used in alignment). Pergolide (Figure 11C) contains a 6-propyl and a $-\text{CH}_2\text{SCH}_3$ group (see also Figure 1). From the CoMFA-constrained pergolide docking, destabilizing interactions are seen for the 6-propyl group but not for the $-\text{CH}_2\text{SCH}_3$ group. The 6-propyl is unique for this compound and may be the primary contributor to the decreased binding affinity for this compound in comparison with the other ergolines studied. The 6-propyl group docks near the ring nitrogen of the very highly conserved Trp 357 from the fingerprint sequence of helix 6 [W in CWLPFF]. This interaction occurs in the crowded region of a van der Waals contact between the conserved Trp 357 and Cys

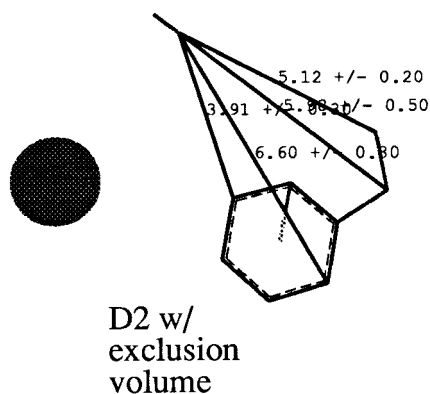


Figure 8. D2 3D search query with added exclusion volume based on CoMFA.

Table 7. Similarity Searches of 3D Hit Lists

D1-Br-APB	sim	D2-lisuride	sim
NCI Hit List			
22185-91-7	0.55	5394-79-6	0.41
25888-41-9	0.54	68219-19-2	0.39
80751-60-5	0.54	6285-23-0	0.38
(next sim = 0.51)		60607-34-3	0.38
		(next sim = 0.37)	
MDDR Hit List			
16766	0.41	14235 ^b	0.63
26	0.41	14234	0.60
(next sim = 0.27)		8984	0.57
		(next sim = 0.53)	
ACD Hit List			
113274 ^a	0.99	100210	0.51
113275	0.99	111819	0.50
(next sim = 0.76)		114908	0.49
		(next sim = 0.46)	
CMC Hit List			
trepipam ^a	0.71	piroxicillin	0.80
fenoldopam	0.66	metionate	0.78
thalicarpine	0.63	saperconazole	0.78
cilobradine	0.61	(next sim = 0.77)	
(next sim = 0.61)			
Maybridge Hit List			
BTB 12808	0.47	NRB 02922	0.38
S01356	0.47	NRB 02921	0.38
(next sim = 0.46)		RDR 0033	0.36
		(next sim = 0.xx)	

^a Shown in accompanying figures. ^a = $E > 10^6$. ^b Bold indicates lisuride enantiomers.

118 of helix 3, one turn deep to the primary ligand binding residue Asp 114. Distances with the Trp 357 are 2.8–3 Å and with Cys118 are close to 1 Å. However, some compounds which we have modeled have a ring to stack between Phe 198 and Phe 361.^{37,39} This allows Trp 357 to assume an alternate favored angle [$\chi^1 = 180^\circ$ and $\chi^2 = 90^\circ$] and to stack between Phe 198 and Phe 361, as was suggested for some piquindone derivatives.³⁹ This would provide much more space for the pergolide 6-propyl group. However, although this space relieves both steric hindrance and partial charge repulsion with the N of Trp 357, the pocket that remains is expected to contain some water molecules, which would still be associated with decreased affinity found for this hydrophobic portion of the pergolide molecule. The $-\text{CH}_2\text{-SCH}_3$ moiety of the docked pergolide sits in a loose pocket between helices 6 and 7. This pocket is lined by the side chain of Phe 360 of helix 6 [the first F in CWLPFF] and two residues of helix 7, Tyr 379 and Phe 382. van der Waals surfaces are complimentary and

hydrophobic and there appears to be no significant partial charge involved, either in the drug or in the receptor regions that form the pocket. Bromocriptine also has a substitution in this position (Figure 11D), suggesting that the substitution may not be that destabilizing to binding of either compound.

Discussion

The major goal was to determine the extent to which CoMFA-derived models of recombinant D1 and D2 DA receptors differed for the same set of DA agonists, a differential QSAR. Differences in pharmacophore maps, especially for the highest affinity compounds, and in the contour maps for agonist affinity at the two receptors were observed. These differences may reflect real underlying differences in the interaction of agonists with the two DA receptor subtypes for the following reasons. First, 3D chemical database searches based on queries derived from the two models yielded hit lists which were quite different from one another while being comprehensive enough to identify training set compounds or their enantiomers. Second, affinity predictions of two additional drugs (apomorphine and 7-OH-DPAT) based on the two CoMFA models were accurate (compared to measured affinities) and quite different for D1 vs D2. Third, the very high D2 (but not D1) affinity of several ergoline compounds in the training set was consistent with dramatic differences in docking between these compounds and of DA itself to the D2 receptor. Together with the very different alignments of catecholamine and ergoline compounds to the two receptors, this latter observation is also consistent with differences in agonist binding modes to D1 and D2.

Our results confirm our previous findings²⁰ that optimal agonist binding to the D1 receptor may require a significantly greater distance between the plane of the ring and the position of the cationic nitrogen than that previously suggested by standard SAR for optimal binding to the pharmacologically defined D2 DA receptor.^{23,50} Furthermore, the present findings extend that work by a direct demonstration that the plane height of the same set of compounds is generally reduced when binding to the recombinant D2 DA receptor (Tables 2 and 3). The present results confirm a previously suggested rationale²⁰ for the historic difficulty of developing D1-selective agonists. Thus, compounds with sufficient flexibility to achieve the plane height optimal for D1 binding could generally assume a flatter configuration consistent with high D2 affinity, unless conformational constraints are present by design. Because greater plane height seems to be consistent with high D1 affinity, this means that when such compounds are flexible, they can also assume a planar conformation and bind well to D2 receptors. However, the converse may not be true, since some compounds may not be able to achieve the needed D1 plane heights without bond breakage. It is of interest that several of the training set compounds seem to assume different conformations when binding to D1 and D2 receptors. In contrast to the differences in plane height, the present results extend our previous results concerning the distance between the primary H-bond site (the meta hydroxyl on the catechol ring or the hydrogen-bonding nitrogen on the five-carbon ring in ergolines) and cationic nitro-

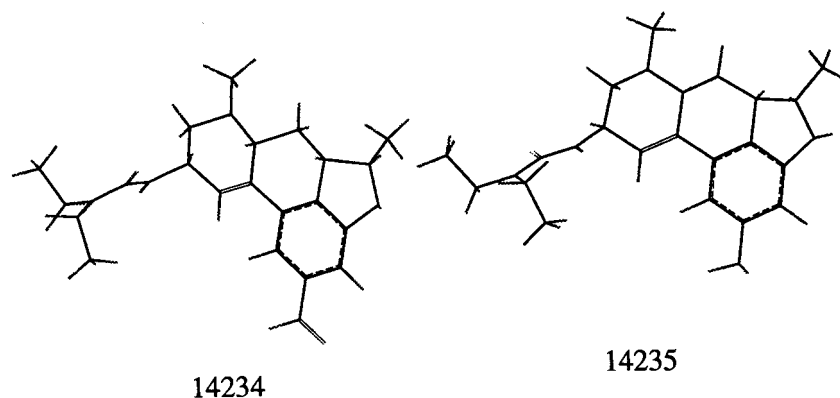


Figure 9. Lisuride enantiomers discovered from 3D search and similarity search.

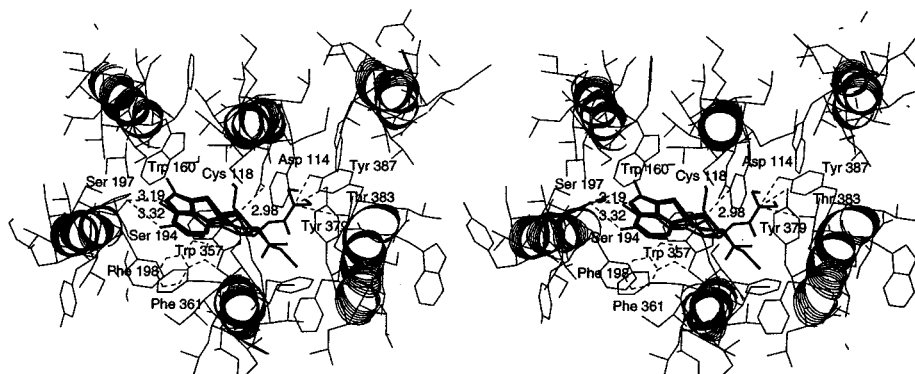


Figure 10. Stereoview of docked ligands in the dopamine D2 receptor. View of helices 2–7 of the D2 receptor with ergolines and dopamine docked. Alignment of docked drugs matches the CoMFA model. Distances between the ligands and the key residues Ser 194 and Asp 114 of the receptor are noted. Trp 357 of helix 6 [CWLPPF] is shown in the bottom center in two conformations, one in solid lines and the other in dotted lines. The solid line conformation matches the Trp in the published dopamine D2 receptor model, with tricyclic antagonists docked. The dotted line conformation is postulated for piquindone derivatives (ref 39). The latter conformation has the Trp stacked between the Phe 198 of helix 5 and Phe 361 of helix 6, whereas in the former tricyclic antagonists are stacked between the Phe residues (ref 37).

gen required for optimal binding. For the highest affinity compounds in the training set, this distance at the D1 receptor is comparable to the corresponding distance between the carbon of the five-membered ring meta to the cationic nitrogen for the D2 receptor (Tables 2 and 3).

The predictive utility of the CoMFA model for two dopaminergic agonists not in the training set (APO and 7-OH-DPAT) was quite good. Thus, at D1 receptors, the predicted K_L value for apomorphine was $0.24 \mu\text{M}$ vs a measured value of $0.22 \mu\text{M}$; the predicted value for 7-OH-DPAT was $17.9 \mu\text{M}$ vs a measured value of $13.0 \mu\text{M}$. For the D2 receptor, there was also good correspondence between the predicted and measured values for the two test compounds. The apomorphine predicted value was $1.07 \mu\text{M}$, whereas the apomorphine measured value was $1.19 \mu\text{M}$. For 7-OH-DPAT, the D2 predicted value was $0.8 \mu\text{M}$, while the 7-OH-DPAT measured value was $0.94 \mu\text{M}$. Together with the structural diversity of the training set compounds, these results suggest that the CoMFA-derived D1 and D2 receptor models may have utility for predicting affinities of novel agonists at each receptor subtype.

Whereas pharmacophore maps derived from alignments based on flexible field fit procedures are primarily useful as starting points for CoMFA, they can also provide some potential insight about key features of agonist binding which may be important for affinity. Because of this practical utility, pharmacophore maps

together with CoMFA-derived exclusion volumes offer particularly useful search queries for 3D chemical databases. The use of UNITY to perform flexible 3D searches based on the pharmacophore maps and CoMFA information was conducted for two reasons in the present report. First, it was of interest to utilize the hit lists derived from each query as a *fingerprint* with which to compare the differences between the pharmacophore maps from which the CoMFA models were derived. The results showed that both queries were (a) internally consistent (could retrieve the compounds used to derive them), (b) robust (yielding reasonable numbers of hits which could easily be prioritized using the SYBYL similarity index), and (c) mutually exclusive (few common hits between D1- and D2-derived hit lists). Thus, the 3D search results indicated that the two pharmacophore maps (Figure 3) and CoMFA models (Figures 5 and 6) were distinct. The second obvious major goal of a 3D search is to generate *new lead compounds*. The present results were intuitively satisfying in that either training set compounds (fenoldopam for D1) or enantiomers of training set compounds (two lisuride enantiomers for D2, Figure 9) were among the hits generated. Furthermore, addition of a CoMFA-derived exclusion volume to the original D2 hit list for the five databases substantially reduced the number of hits, as expected (Table 6 and Figure 8). Also, the reasonable number of hits derived from the queries suggested that they were not unduly restrictive. Fi-

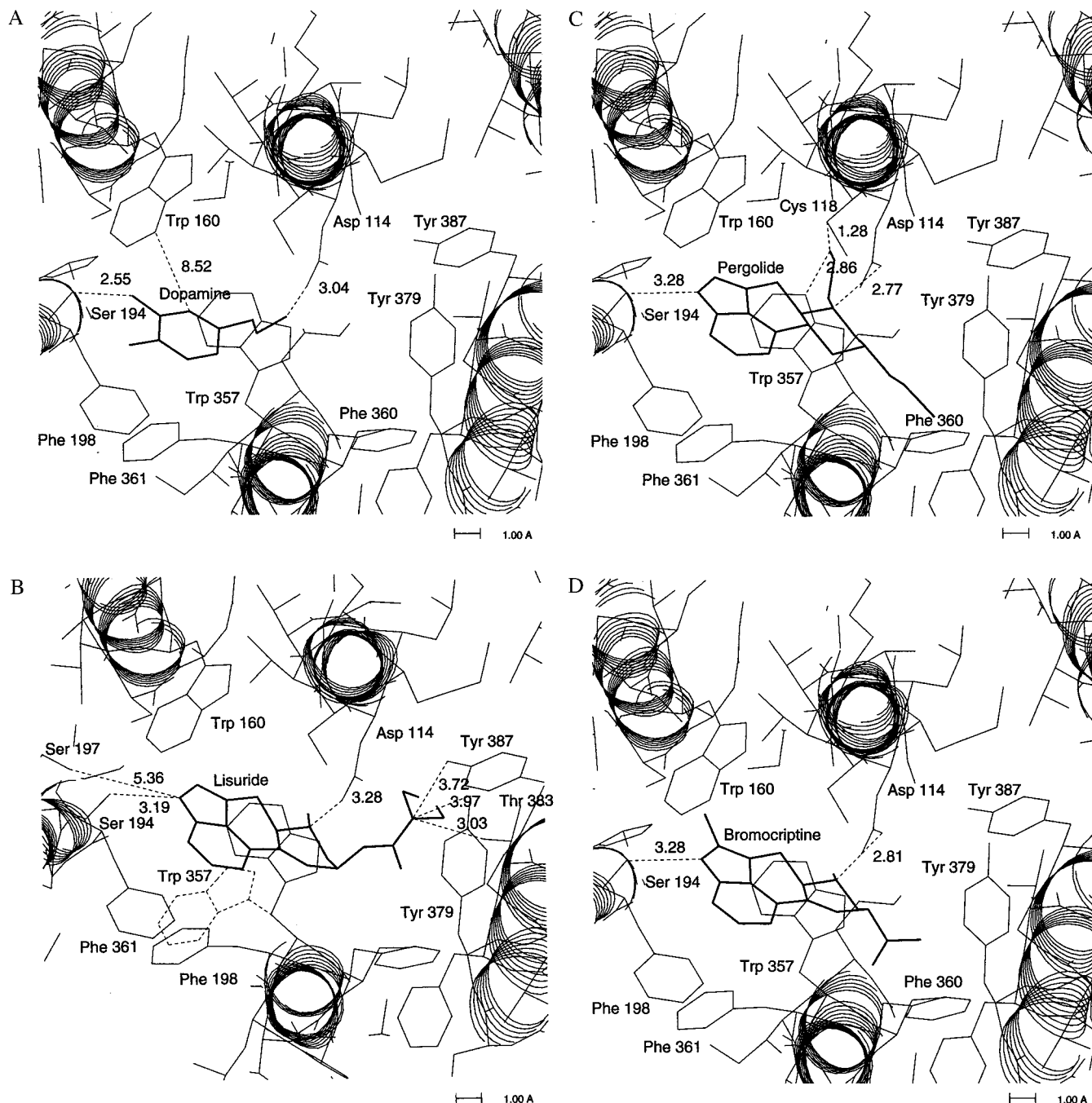


Figure 11. Close up view of the D2 receptor model with each of four agonists docked (A–D). The figure is viewed from outside the cell membrane through the putative entry channel. Helix numbers starting at 2:00 counterclockwise are 2, 3, 4 on the top and 5, 6, 7 on the bottom. Panel A: dopamine docked. Both dopamine hydroxyls are within hydrogen-bonding distance of Ser 194 (see text), as is the cationic nitrogen distance to Asp 114. Note the large distance between dopamine and Trp 160, which lines the binding pocket. Panel B: lisuride docked. Reasonable distances from the cationic nitrogen of lisuride to Asp 114 and from the nitrogen of the five-membered ring to Ser 194 are found. The distance from this nitrogen to Ser 197 of helix 5 [$d = 5.36$ Å] is too great to permit hydrogen bond formation. Note potential interactions with the cationic diethyl urea nitrogen. Panel C: pergolide docked. Note the destabilizing interactions for the 6-propyl group, but not for the $-\text{CH}_2\text{SCH}_3$ group, near Phe 360. Panel D: bromocriptine docked. Note the satisfactory bonding of the N in the five-membered ring to Ser 194 as well as that of the cationic nitrogen to Asp 114.

nally, the combination of the SYBYL similarity index with the UNITY-based hit list allowed a convenient rank ordering of the new compounds based on their resemblance to a high-affinity compound within the original training set.

One goal of the present study was to compare our previously published^{37,39} docking of agonist structures to the D2 receptor with docking of CoMFA-derived structures to the same receptor. A favorable docking

of the CoMFA-derived agonist structures with key residues of the D2 receptor was found. This docking appears to rationalize the ergoline agonist affinity data and correlates well overall with the CoMFA. An important observation was the different binding modes for DA vs the highest affinity ergoline compounds. This can be seen for the basic region of the contour plot for the D2 receptor adjacent to the cationic nitrogen, which may come from the diethyl urea group of lisuride (Figure

11, panel A vs panel B). However, there are still some unfavorable van der Waals contacts remaining with the agonists. The remaining high-energy regions point out the possible conformational flexibility of the agonists as well as the fact that the D2 receptor model can be further refined. The fact that the affinity data can be correlated with the CoMFA and the receptor model, however, validates both entirely independent procedures.

Together, the present studies enhance the information available about agonist interactions with D1 and D2 dopamine receptors available from molecular cloning,^{51–56} protein modeling,^{57,58} and classical studies with drug enantiomers.⁵⁹ In particular, the use of the same training set of structurally diverse agonists to predict affinities measured at recombinant DA receptor subfamilies allows a more direct comparison of the computational chemistry models than has previously been possible, a differential QSAR. Furthermore, the comparison of presumed drug binding conformations derived from CoMFA vs docking with a protein homology model represents a novel extension of computational chemistry methodology.

Acknowledgment. This work was supported in part by NIH (RR08579A), U.S. EPA (HRCCLS-Sub-UT-4/9/93), TRIPOS Inc., and Glaxo Inc., and by the Department of Veterans Affairs Merit Review and Career Scientist Programs. Additional funding was provided by a grant from a schizophrenia research fund at the ENRM VA Medical Center in Bedford, MA (to C.J.D. and M.M.T.). In addition, the support of Greg Binus, M.D., Chief of Psychiatry Service at VA Bedford, is gratefully acknowledged.

References

- Strange, P. G. *Brain biochemistry and brain disorders*; Oxford University Press: New York, 1993.
- Waddington, J. *D1/D2 Dopamine receptor interactions*; Academic Press: New York, 1993.
- Wilcox, R. E.; Gonzales, R. A.; Joseph D. Miller. Introduction to neurotransmitters, receptors, signal transduction, and second messengers. Chapter 1 in *Textbook of Psychopharmacology*, 2nd ed.; Nemeroff, C. B., Schatzberg, A. F., Eds.; American Psychiatric Press: Washington, DC, in press.
- Wilcox, R. E.; Gonzales, R. A. Introduction to neurotransmitters, receptors, signal transduction and second messengers. Chapter 1 in *Textbook of Psychopharmacology*; Nemeroff, C. B., Schatzberg, A. F., Eds.; American Psychiatric Press: Washington, DC, 1995; pp 3–31.
- Neve, K. A.; Neve, R. L., Eds. *The Dopamine Receptors*; Humana Press: Clifton, NJ, 1997.
- Sibley, D. R.; Monsma, F. J., Jr. Molecular biology of dopamine receptors. *Trends Pharmacol. Sci.* **1992**, *13*, 61–69.
- Lieberman, J.; Koreen, A. Neurochemistry and neuroendocrinology of schizophrenia: a selective review. *Schiz. Bull.* **1993**, *19*, 371–429.
- Rogers, J.; Bloom, F. E. Neurotransmitter metabolism and function in the aging central nervous system. In *Handbook of The Biology of Aging*; Finch, C. E., Schneider, E. L., Eds.; Van Nostrand Reinhold Company: New York, 1985; pp 645–665.
- Rowland, L. S. *Merritt's textbook of neurology*, 9th ed.; Williams & Wilkins: Baltimore, 1995.
- Civelli, O.; Bunzow, J. R.; Grandy, D. K. Molecular diversity of the dopamine receptors. *Annu. Rev. Pharmacol. Toxicol.* **1993**, *32*, 281–307.
- Civelli, O.; Bunzow, J. R.; Grandy, D. K.; Zhou, Q.-Y.; Van Tol, H. H. M. Molecular biology of the dopamine receptors. *Eur. J. Pharmacol. - Mol. Pharmacol. Sec.* **1991**, *207*, 277–286.
- Gingrich, J. A.; Caron, M. G. Recent advances in the molecular biology of dopamine receptors. *Ann. Rev. Neurosci.* **1993**, *16*, 299–321.
- Machida, C. A.; Searles, R. P.; Nipper, V.; Brown, J. A.; Kozell, L. B.; Neve, K. A. Molecular cloning and expression of the rhesus macaque D1 dopamine receptor gene. *Mol. Pharmacol.* **1992**, *41*, 652–659.
- O'Dowd, B. F. Structures of dopamine receptors. *J. Neurochem.* **1993**, *60*, 804–816.
- Dearry, A.; Gingrich, J. A.; Falardeau, P.; Freneau, R. T., Jr.; Bates, M. D.; Caron, M. G. Molecular cloning and expression of the gene for a human D₁ dopamine receptor. *Nature* **1990**, *347*, 72–76.
- Hibert, M. F.; Trump-Kallmeyer, S.; Bruinvels, A.; Hoflack, J. Three-dimensional models of neurotransmitter G-binding protein-coupled receptors. *Mol. Pharmacol.* **1991**, *40*, 8–15.
- Cramer, R. D., III; Depriest, S.; Patterson, D.; Hecht, P. The developing practice of comparative molecular field analysis. In *3D QSAR in Drug Design - Theory, methods, and applications*; Kubinyi, H., Ed.; ESCOM: Leiden, 1993; pp 443–485.
- Green, S. M.; Marshall, G. R. 3D-QSAR: a current perspective. *Trends Pharmacol. Sci.* **1995**, *16*, 285–291.
- Alkorta, I.; Villar, H. Considerations on the recognition of the D1 receptor by agonists. *J. Comput.-Aided Mol. Des.* **1993**, *7*, 659–670.
- Brusniak, M.-Y. K.; Pearlman, R. S.; Neve, K. A.; Wilcox, R. E. Comparative molecular field analysis-based prediction of drug affinity at recombinant D1A dopamine receptors. *J. Med. Chem.* **1996**, *39*, 850–859.
- Dunn, W. J.; Wold, S.; Edlund, V.; Helberg, S. Multivariate structure-activity relationships between data from a battery of biological tests and an ensemble of structure descriptors: the PLS method. *Quantum Struct.-Act. Relat.* **1984**, *3*, 131–137.
- Kozell, L. B.; Machida, C. A.; Neve, R. L.; Neve, K. A. Chimeric D1/D2 dopamine receptors. Distinct determinants of selective efficacy, potency, and signal transduction. *J. Biol. Chem.* **1994**, *269*, 30299–30306.
- Seeman, P. Brain dopamine receptors. *Pharmacol. Rev.* **1980**, *32*, 229–313.
- CONCORD User's Manual Version 3.0.1. TRIPOS, Inc.: St. Louis, MO, March 1993.
- SYBYL User's Manual Version 6.4. TRIPOS, Inc.: St. Louis, MO, 1998.
- Kozell, L. B.; Neve, K. A. Constitutive activity of a chimeric D2/D1 dopamine receptor. *Mol. Pharmacol.* **1997**, *52*, 1137–1149.
- Agarwal, A.; Taylor, E. W. 3-D QSAR for intrinsic activity of 5-HT_{1A} receptor ligands by the method of comparative molecular field analysis. *J. Comput. Chem.* **1993**, *14*, 237–245.
- Langlois, M.; Bremont, B.; Rousselle, D.; Gaudy, F. Structural analysis by the comparative molecular field analysis method of the affinity of β -adrenoreceptor blocking agents for 5-HT_{1A} and 5-HT_{1B} receptors. *Eur. J. Pharmacol. - Mol. Pharmacol. Sec.* **1993**, *244*, 77–87.
- Bunzow, J.; VanTol, H.; Grandy, D.; Albert, P.; Salon, J.; Christie, M.; Machida, C.; Neve, K. A.; Civelli, O. Cloning and expression of a rat D2 dopamine receptor cDNA. *Nature* **1988**, *336*, 783–787.
- Severson, J. A.; Wilcox, R. E. Agonist binding to striatal dopamine receptors in aging: the ternary complex of receptor and guanine nucleotide binding regulatory protein. *Ann. N. Y. Acad. Sci.* **1988**, *524*, 67–77.
- Seeman, P.; Niznik, H. B. Dopamine D₁ receptor pharmacology. *ISI Atlas Sci.* **1988**, 161–170.
- Brewster, W. K.; Nichols, D. E.; Riggs, R. M.; Mottola, D.; Lovenberg, T. W.; Lewis, M. H.; Mailman, R. B. trans-10,11-dihydroxyl-5,6,6a,7,8,12b-hexahydrobenzo[a]phenanthridine: a highly potent selective dopamine D1 full agonist. *J. Med. Chem.* **1990**, *33* (6), 1756–1764.
- Cox, B. A.; Henningsen, R. A.; Spanoyannis, A.; Neve, R. L.; Neve, K. A. Contributions of conserved serine residues to the interactions of ligands with dopamine D2 receptors. *J. Neurochem.* **1992**, *59*, 627–635.
- Livingstone, C. D.; Strange, P. G.; Naylor, L. H. Molecular modeling of D₂-like dopamine receptors. *Biochem. J.* **1992**, *287*, 277–282.
- Pollock, N. J.; Manelli, A. M.; Hutchins, C. W.; Steffey, M. E.; MacEnzie, R. G.; Frail, D. E. Serine mutations in transmembrane V of the dopamine D₁ receptor affect ligand interactions and receptor activation. *J. Biol. Chem.* **1992**, *267*, 17780–17786.
- Pearlman, R. S. Rapid generation of high-quality approximate 3D molecular structures. *Chem. Design Auto. News* **1987**, *2*, 1–9.
- Teeter, M. M.; Froimowitz, M.; Stec, B.; DuRand, C. J. Homology modeling of the dopamine D2 receptor and its testing by docking of agonists and tricyclic antagonists. *J. Med. Chem.* **1994**, *37*, 2874–2888.
- Dewar, M.; Thiel, W. Ground states of molecules. 38. The MNDO method. Approximation and parameters. *J. Am. Chem. Soc.* **1977**, *99*, 4899–4917.
- Teeter, M. M.; DuRand, C. J. Dopamine D₂ Receptor Model Explains Binding Affinity of Neuroleptics: Piquindone and its Structure Activity Relationships. *Drug Des. Discovery* **1996**, *13*, 49–62.
- Hutchins, C. Three-dimensional models of the D1 and D2 dopamine receptors. *Endocrine J.* **1994**, *2*, 7–23.

- (41) Marshall, G. R.; Barry, D. C.; Bosshard, H. E.; Dammkoehler, R. A.; Dunn, D. A. The conformational parameter in drug design: the active analog approach. In *Computer-Assisted Drug Design*; Olsen, E. C., Christoffersen, R. E., Eds.; ACS Symposium Series 112; American Chemical Society: Washington, DC, 1979; pp 205–226.
- (42) Martin, Y. C.; Bures, M. G.; Danaher, E. A.; DeLazzer, J.; Lico, I.; Pavlik, P. A. A fast new approach to pharmacophore mapping and its application to dopaminergic and benzodiazepine agonists. *J. Comput.-Aided Mol. Des.* **1993**, *7*, 83–102.
- (43) Martin, Y. C. A practitioner's perspective of the role of quantitative structure–activity analysis in medicinal chemistry. *J. Med. Chem.* **1981**, *24*, 229–237.
- (44) Martin, Y. C. Computer-assisted rationale drug design. *Methods Enzymol.* **1991**, *203*, 587–613.
- (45) Charifson, P.; Bowen, P.; Wyrick, S.; Hoffman, A.; Cory, M.; McPhail, A.; Mailman, R. Conformational analysis and molecular modeling of 1-phenyl-, 4-phenyl, and 1-benzyl-1,2,3,4-tetrahydroisoquinolines as D1 receptor ligands. *J. Med. Chem.* **1989**, *32*, 2050–2058.
- (46) Starr, S.; Wiens, B.; Neve, K. A.; Pearlman, R. S.; Wilcox, R. E. Molecular basis for agonist selectivity at dopamine D1 and D2 receptors. *Soc. Neurosci. Abstr.* **1995**, *21* (#252.11), 619.
- (47) Pearlman, R. S. 3D Molecular structures: generation and use in 3D searching. In *3D QSAR in drug design—theory, methods, and applications*; Kubinyi, H., Ed.; ESCOM Science Pub.: Leiden, 1993; pp 41–79.
- (48) Mak, C.; Avalos, M.; Randall, P. K.; Whisenand, R.; Kwan, S.-W.; Abell, C. W.; Wilcox, R. E. Clonal cell lines stably expressing recombinant receptors: ideal systems for determining agonist affinity and efficacy. *Neuropharmacology* **1996**, *35* (5), 549–570.
- (49) Wilcox, R. E.; Mak, C.; Avalos, M.; Randall, P.; Whisenand, R.; Kwan, S.-W.; Abell, C.; Neumeyer, J. Relative intrinsic efficacy and functional affinity constants of drugs in C6 glioma cells stably expressing the D1 dopamine receptor. *Soc. Neurosci. Abstr.* **1992**, *19* (#38.5), 75.
- (50) Seeman, P. Dopamine receptor sequences. Therapeutic levels of neuroleptics occupy D2 receptors, clozapine occupies D4. *Neuropsychopharmacology* **1992**, *7*, 261–284.
- (51) Jarvie, K. R.; Tiberi, M.; Silvia, C.; Gingrich, J. A. Molecular cloning, stable expression and desensitization of the human dopamine D1B/D5 receptor. *J. Receptor Res.* **1993**, *13*, 573–590.
- (52) Sokoloff, P.; Giros, B.; Martres, M.-P.; Bouthenet, M.-L.; Schwartz, J.-C. Molecular cloning and characterization of a novel dopamine receptor (D3) as a target for neuroleptics. *Nature* **1990**, *347*, 146–151.
- (53) Monsma, F. J., Jr.; Mahan, L. C.; McVittie, L. D.; Gerfen, C. R.; Sibley, D. R. Molecular cloning and expression of a D1 dopamine receptor linked to adenylyl cyclase activation. *Proc. Natl. Acad. Sci. U.S.A.* **1990**, *87*, 6723–6727.
- (54) Sunahara, R. G.; Niznik, H. B.; Weiner, D. M.; Stormann, T. M.; Brann, M. R.; Kennedy, J. L.; Gelernter, J. E.; Rozmahel, R.; Yang, Y.; Israel, Y.; Seeman, P.; O'Dowd, B. F. Human dopamine D1 receptor encoded by an intronless gene on chromosome 5. *Nature* **1990**, *347*, 80–83.
- (55) Tiberi, M.; Jarvie, K.; Silvia, C.; Falardeau, P.; Gingrich, J.; et al. Cloning, molecular characterization and chromosomal assignment of a gene encoding a novel D1 dopamine receptor subtype: differential expression pattern in rat brain compared to the D1 receptor. *Proc. Natl. Acad. Sci. U.S.A.* **1991**, *88*, 8111.
- (56) Zhou, Q.-Y.; Grady, D.K.; Thambi, L.; Kushner, J. A.; Van Tol, H. H. M.; Cone, R.; Pribnow, D.; Salon, J.; Bunzow, J. R.; Civelli, O. Cloning and expression of human and rat D1 dopamine receptors. *Nature* **1990**, *347*, 76–79.
- (57) Dahl, S. G.; Edvardsen, Ø.; Sylte, I. Molecular dynamics of dopamine at the D₂ receptor. *Proc. Natl. Acad. Sci. U.S.A.* **1991**, *88*, 8111–8115.
- (58) Moereels, H.; Leysen, J. E. Novel computational model for the interaction of dopamine with the D2 receptor. *Recept. Channels* **1993**, *1*, 89–97.
- (59) Goldman, M. E.; Keababian, J. W. Aporphine enantiomers. Interactions with D-1 and D-2 dopamine receptors. *Mol. Pharmacol.* **1984**, *25*, 18–23.
- (60) In the original version of the manuscript we had selected the highly rigid compound, DHX, as the D1 template. However, on the basis of a suggestion by one of the reviewers, we repeated the alignment and CoMFA for the D1 model using the higher affinity, but less conformationally constrained, compound Br-APB as template.
- (61) Generally, alignment of most of the training set compounds with catechol-like structures was quite good with Br-APB, whereas alignment of the ergoline compounds was more problematic. Similarly, alignment of the training set compounds possessing ergoline features with bromocriptine was generally excellent; in contrast, alignment of the catechol-like compounds was less successful. The strategy that seemed most successful empirically was to take the compound of the dissimilar structural class which had the smallest residual value in the initial CoMFA and use it as a pseudo template to improve the alignment of structurally related compounds.
- (62) Partial least squares uses of CoMFA properties of the training set compounds to regress the target property (affinity). The analysis incorporates the factor analysis method of principal component analysis in order to detect simple linear relationships among the CoMFA variables which can account for affinity. Generally, factor analytic methods accomplish this by performing a multidimensional rotation on the table of CoMFA data. The goal of a principal component analysis (a factor analysis without rotation) is to find a new orthogonal coordinate system so that the variance of the training set data with respect to the new axes are maximized in decreasing order (first coordinate describes the maximum variance, second coordinate describes the next largest variance, etc.). The principal components are the eigenvectors of the correlation matrix of the data.²⁵
- (63) The predictions discussed were obtained using earlier versions of the two CoMFA models, which yielded similar q^2 values to the models reported here. Also, the pharmacophore maps used to assist in developing the search queries were very similar to those associated with the final models. It is important to note that these good predictions occurred only with conformers of the two compounds which were well fit to the template compound for each CoMFA. Other conformers or those less well fit had predicted values which deviated to a significantly greater extent from the measured values (data not shown).
- (64) 3D database searches were done using search queries derived from earlier versions of the two CoMFA models, which were similar in key distances and plane heights to those of the final model and which had similar q^2 values.
- (65) One of the reviewers suggested that we obtain these two compounds and measure their affinities. Unfortunately, Schering had already discontinued testing with them, and we were unable to obtain them.
- (66) In the D1 receptor, the corresponding residues are Phe, Val, and Trp, with no potential hydrogen-bonding oxygens available.

JM9800292